Catalysis
Science &
Technology

This article can be cited before page numbers have been issued, to do this please use: W. Fu, Y. Xu, L. Zeng, Z. Fu, C. Li, Z. Yang and . , *Catal. Sci. Technol.*, 2018, DOI: 10.1039/C8CY00138C.

View Article Online
DOI: 10.1039/C8CY00138C

Journal Name

ARTICLE

Photocatalytic oxidation of arylalcohols to aromatic aldehydes promoted by hydroxyl radicals over CoP/CdS photocatalyst in water with hydrogen evolution†

Received 00th January 20xx,
Accepted 00th January 20xx

DOI: 10.1039/x0xx00000x

www.rsc.org/

Yong Xu,[a,b‡] Ling-Zhen Zeng,[c‡] Zhi-Cheng Fu,[a] Cong Li,[c] Zhi Yang,[c] Yong Chen[a] and Wen-Fu Fu*[a,c]

The cobalt phosphide (CoP) combined with CdS was employed as a photocatalyst to oxidize arylalcohols into aromatic aldehydes or ketones in water. This was accompanied by the reduction of water, and hydrogen evolution was much more than the chemical equivalent of hydrogen gas. Electron spin resonance spectroscopy and quenching experiments demonstrated that hydroxyl free radicals, originating from water splitting, promoted the oxidation of arylalcohols, while holes in the valence band of the photocatalyst were reduced by the $^{-}$OH and organic substrates. The overall reaction generates high-value-added organics. This photocatalytic reaction is atom-economical, in accordance with the concept of sustainable development.

1. Introduction

Utilization of solar energy to drive chemical reactions has received increasing attention, being an energy-saving, effective and green approach.[1-3] In 1972, Fujishima and Honda reported a solar-driven alternative to traditional chemical synthesis.[4] The conversion of alcohols into aldehydes is an important reaction process in both chemical research and industry, being widely used in the production of food, perfumes and pharmaceuticals.[5] The traditional method of transforming alcohols to aldehydes not only uses toxic or caustic oxidants but also requires relatively high pressure and temperature. As an alternative, oxidation of alcohols to aldehydes or ketones by using O_2 has been reported in both homogeneous and heterogeneous catalytic systems.[6,7] Palmisano et al. studied the oxidation of benzyl alcohols by O_2 using TiO_2 as catalyst under ultraviolet light irradiation.[8,9] However, because about 50% of total solar energy is in the visible region of the spectrum, it is necessary to develop visible-light-responsive catalysts. Typical visible-light-responsive semiconductors include dye-sensitized or rare-earth-doped TiO_2, transition metal oxides and sulfides, and carbon nitride.[10-19] Recently, numerous efforts have been made to use O_2 as electron acceptor and Au/CeO_2, Au/TiO_2, CdS-UiO-66(NH_2), or Pt/$BiWO_6$ as photocatalysts under visible-light irradiation.[20-27] However, if a system were developed in which the electrons of the conduction band were captured by H^+ to produce H_2, this would be an ideal replacement for fossil fuels.

CdS, as a representative type II-VI semiconductor, is deemed a promising candidate for transformation of solar energy into chemical energy on account of its suitable band gap.[1,28] However, the application of pure CdS is circumscribed by the fast recombination of photogenerated electron-hole pairs as well as the propensity to suffer photocorrosion. Therefore, a great many measures have been taken to boost the activity and stability of CdS, among which the combination of CdS with a cocatalyst is particularly simple but effective.[29,30] By promoting rapid electron transfer from CdS into the cocatalyst, the combined system gives rise to efficient and longer-lasting photoinduced charge separation through lessening the recombination of electron-hole pairs. Cobalt phosphide (CoP) is an example of non-noble-metal cocatalysts which exhibits high photocatalytic hydrogen-generating activity when it combined with CdS. The generation rate of hydrogen can reach up to 254,000 μmol h^{-1} g^{-1} under sunlight irradiation.[31] Transition metal phosphides have also been intensively studied as catalysts for hydrodesulfurization, as they possess high electrical conductivity and metalloid characteristics, similarly to zero-valent metals.[32]

In view of the excellent photocatalytic activity of this class of promising materials, we attempted to further extend their applicability to photocatalytic oxidation of organics. Herein we report the use of a composite CoP/CdS material as visible-light catalyst for the oxidation of arylalcohols to aromatic aldehydes or ketones in water. The reaction was accompanied by hydrogen generation, and the quantitative yields of hydrogen evolution were much more than the chemical equivalent of hydrogen gas. It was found that hydroxyl free radicals,

---

‡ These authors contributed equally to this work
[a] Key Laboratory of Photochemical Conversion and Optoelectronic Materials and HKU-CAS Joint Laboratory on New Materials, Technical Institute of Physics and Chemistry, Chinese Academy of Sciences, Beijing 100190, P.R. China
[b] University of Chinese Academy of Sciences, Beijing 100190, P.R. China
E-mail: fuwf@mail.ipc.ac.cn
[c] College of Chemistry and Chemical Engineering, Yunnan Normal University, Kunming 650092, P.R. China

† Electronic Supplementary Information (ESI) available: See DOI:10.1039/x0xx00000x

View Article Online
DOI: 10.1039/C8CY00138C

produced by photoinduced splitting of water, drove the efficient catalytic oxidation of arylalcohols. Electron spin resonance (ESR) spectral and isotope labeling experiments and product analysis provided direct evidence on the mechanistic interpretation and origin of hydrogen evolution.

2. Experimental

2.1 Preparation

2.1.1Preparation of CoP nanoparticles. CoP nanoparticles were prepared through a solid-state thermal phosphorization reaction. Typically, 2.0 g NaOH was added to a 500 mL of aqueous solution containing 594 mg sodium citrate and 2,379 mg $CoCl_2•6H_2O$ in a round-bottom flask. After stirring for 15 min, the generated suspension was separated by centrifugation and washed with a large amount of water. The obtained $Co(OH)_2$ was dried in a vacuum oven at the temperature of 100 °C. After this, 200 mg of oven-dried $Co(OH)_2$ and 1,000 mg NaH_2PO_2 were ground in a mortar to form a uniform mixture, and transferred into a vessel. Then, the vessel was directly heated to 300 °C for 4 h under Ar atmosphere in a tube furnace. Subsequently, the sample was cooled naturally to room temperature in continuous Ar flow. Finally, the obtained black solid was washed with water as well as hydrochloric acid several times and dried in a vacuum oven.

2.1.2 Preparation of CdS nanoparticles. In a typical procedure, 400 mL (0.14 M) of aqueous Na_2S solution was added slowly to 500 mL (0.14 M) of $Cd(OAc)_2$ solution with vigorous stirring. The resulting yellow precipitate was stirred for 24 h and then allowed to settle for 24 h. The yellow slurry was filtered and washed with 200 mL of water, then transferred to a dried Teflon-lined autoclave with a capacity of 100 mL. The autoclave was sealed and heated at 200 °C for 24 h, after which the system was allowed to cool to room temperature naturally. The obtained yellow solid was filtered and then washed with 500 mL of water and 100 mL of ethanol consecutively. After drying at 80 °C for 5 h in the oven, the obtained yellow solid was ground into fine particles.

2.2 Characterization

The samples were characterized by powder X-ray diffraction (XRD) on a Bruker AXS D8 X-ray diffractometer with Cu K_α radiation (λ =1.54056 Å) to identify their phases. The particle size and lattice fringes of the samples were analyzed on a transmission electron microscope (TEM; JEM 2100F) with an accelerating voltage of 200 kV. Ultraviolet-visible diffuse reflectance spectra (DRS) were measured on a spectrophotometer (Hitachi UV-3010) using $BaSO_4$ as a reference. ESR signals were recorded at room temperature with a Bruker ESR E500 spectrometer. The chemical structure and the quantity of the products were determined by ^1H nuclear magnetic resonance (NMR) spectroscopy (BrukerAvance 400 spectrometer). The produced hydrogen was measured by gas chromatography (GC-2014C, Shimadzu, with Ar as a carrier gas) with a 5 Å molecular sieve column (3 m × 2 m) and a thermal-conductivity detector.

2.3 Photoelectrochemical (PEC) measurements

Photocurrent measurements were conducted on a CHI 660e electrochemical workstation (Chenhua Instrument, China) using a conventional three-electrode configuration. A catalyst electrode served as the working electrode, with a platinum foil as the counter electrode and an Ag/AgCl (saturated KCl) electrode as the reference electrode. Then, 0.2 M of Na_2SO_4 aqueous solution (pH = 6.8) was used as the electrolyte, through which N_2 was bubbled for 20 min prior to measurement. A white light-emitting diode (LED) (30 × 3 W, λ ≥ 420 nm) light source was used for irradiation. The working electrodes were prepared as follows: 3 mg of sample was dispersed in 40 μL isopropanol with 5 μL Nafion by sonication for 20 min. The slurry was then evenly spread onto a 3.0 × 1.0 cm^2 conducting indium tin oxide glass substrate with an active area of about 1.0 cm^2. The film was dried in air. The photoresponses of the samples with the light on and off were measured at 0.0 V. Electrochemical impedance spectroscopy (EIS) measurementswere carried out using an AC amplitude of 10 mV in the frequency range of 0.01 Hz–1000 kHz at 0.05 V.

2.4 Photocatalytic test

Typically, 5 mL of water containing 0.1 mmol substrate and 2.5 mg CoP/CdS photocatalyst was added to a 15 mL cuvette sealed with a rubber septum placed on top of a magnetic stirrer. A stream of N_2 was then passed into the reaction system for 10 min. White LEDs (30 × 3 W, λ ≥ 420 nm) were used as the irradiation light source. The LEDs were positioned 3 cm away from the sample, which was kept under continuous stirring at room temperature. The mixture was stirred for 30 min before irradiation.

3. Results and discussion

3.1 Characterization of photocatalysts

CoP was prepared by a solid-state thermal phosphorization reaction.[31] Its TEM and high-resolution TEM (HRTEM) images are depicted in Fig. S1 in the electronic supplementary information (ESI†). Fig. 1a shows the XRD pattern of the prepared orthorhombic CoP nanoparticles (JCPDS 29-0497), with no impurity peaks. Five distinct diffraction peaks at about 31.7°, 36.5°, 46.3°, 48.4° and 56.6° can be seen, corresponding to the (011), (111), (112), (211) and (301) reflections of the CoP phase, respectively. The hexagonal CdS nanospheres (JCPDS 65-3414) were synthesized according to a conventional method (Fig. S2 and S3†).[28] The CoP/CdS composite material was obtained via grinding CoP nanoparticles and CdS nanospheres together in a mortar to obtain uniformity. The XRD pattern (Fig. 1b) shows no obvious peaks of CoP after loading 5 wt% CoP on the as-prepared CdS. This may be because the peak intensity of CoP is much weaker than that of CdS, and CoP is highly dispersed in the CdS nanospheres. Fig.

View Article Online
DOI: 10.1039/C8CY00138C

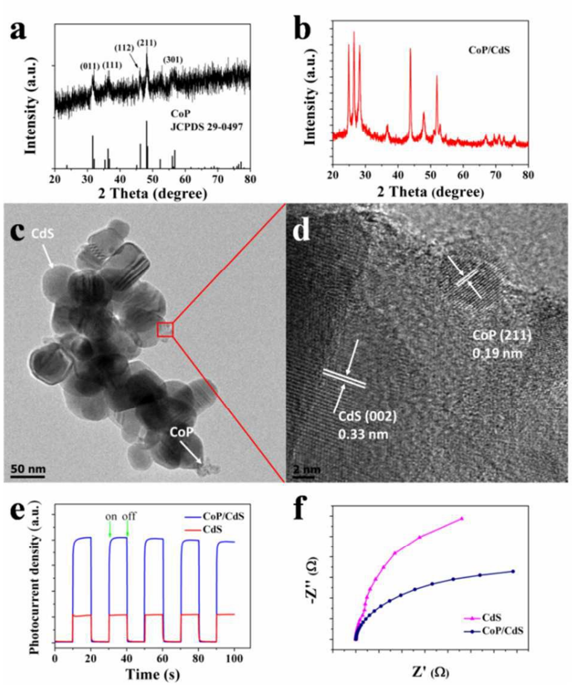

Fig. 1 (a) XRD patterns of CoP and (b) CoP/CdS, (c) TEM and (d) HRTEM images of CoP/CdS(5 wt%), (e) transient photocurrent response under visible-light irradiation, (f) EIS Nyquist plots of CdS and CoP/CdS (5 wt%).

1c shows TEM images of the 5 wt% CoP/CdS photocatalyst, which confirms that the CoP nanoparticles are polydispersed. As shown in the HRTEM image (Fig. 1d), the CoP nanoparticles are less than 10 nm in diameter, and the lattice fringes with spacings of 0.19 and 0.33 nm correspond to the (211) and (002) planes of CoP and CdS, respectively. The transient photocurrent responses of CdS and CoP/CdS showed that charge transfer was more efficient for the latter, thereby suppressing charge recombination as well as lengthening the lifetime of charge carriers (Fig. 1e). It can be seen from the EIS Nyquist plots that the impedance radius is smaller for CoP/CdS than for pure CdS, which further confirms the decrease of charge transfer resistance on the surface of the former (Fig. 1f). Ultraviolet-visible DRS of the as-synthesized samples were shown in Fig. S4. In comparison with the band gap of the CdS (2.18 eV), that of CoP/CdS is approximately 2.23 eV. Thus, the formation of a CoP@CdS may efficiently promote conversion of solar energy.

3.2 Photocatalytic oxidation of arylalcohols

Photodriven oxidation was carried out in aqueous solution under anaerobic conditions at room temperature. The chosen substrate was 4-methylbenzyl alcohol, which has a distinct ^1H NMR spectrum, and can be accurately weighed because it is a solid. In a typical process, 5 mL of aqueous solution containing 4-methylbenzyl alcohol (0.1 mmol) and photocatalyst (CoP/CdS) in a 15 mL cuvette was irradiated by a white light LED (λ > 420 nm) under N_2 atmosphere with magnetic stirring. The resulting mixture was extracted thoroughly using dichloromethane as extraction agent, and the extracted liquid was dried with anhydrous Na_2SO_4. The chemical structures and the quantity of products were confirmed via ^1H NMR spectroscopy. Control experiments showed that photocatalyst, light and substrate were all indispensable for the photocatalytic oxidation reaction (Fig. 2a). The conversion was only 1.7% in the absence of CoP. However, when the photocatalyst CoP/CdS (5 wt%) was added into the aqueous solution, the conversion reached 88.0% with 109.1 μmol hydrogen evolution. In anhydrous acetonitrile, no oxidation product or hydrogen gas was detected (Fig. S5†). These results showed that water plays a crucial role in this catalytic system. To further understand the reaction process, D_2O was used in place of H_2O. Under these conditions, D_2 was detected by gas chromatography with He as carrier gas (Fig. S6†), indicating that the H_2 detected in the main experiment originated from water. The molar ratio between produced H_2 and the theoretical H_2 generation, including the main product aldehyde and the byproducts, was calculated to be 109.1:98.1. This clearly showed that although the amount of hydrogen production is directly related to the extent of arylalcohol oxidation, the partial contribution of all the water splitting to total amounts of hydrogen can not be excluded. The content of CoP has a great influence on the efficiency of photocatalytic oxidation. Fig. 2b compares the photocatalytic activity of hydrogen generation at different ratios of CoP/CdS (1 wt%, 2.5 wt%, 5 wt% and 10 wt%). With increasing CoP concentration in the range from 1 wt% to 5 wt%, the production of hydrogen gradually rose. The reason for this was the exposure of more active sites, resulting in higher catalytic activity. However, the amount of produced hydrogen fell when the content of CoP was further increased to 10 wt%. This can be tentatively

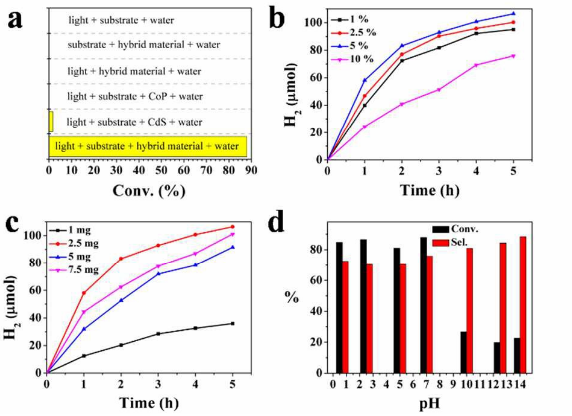

Fig. 2 (a) Control experiments of photocatalytic reactions; (b) the influence of CoP content on hydrogen production; (c) dependence of hydrogen production on dosage of catalyst and irradiation time; (d) the impact of pH on photocatalytic activity (CoP/CdS 5 wt%). Reaction conditions: 2.5 mg catalyst, 5 mL of water, 4-methylbenzyl alcohol (0.1 mmol), visible-light irradiation for 5 h at room temperature.

View Article Online
DOI: 10.1039/C8CY00138C

attributed to the greater coverage of CoP nanoparticles on the surface of CdS, partly hindering the absorption of visible light. Therefore, the optimum loading amount of CoP is 5 wt% in the present study. The dosage of photocatalyst also has a significant impact on conversion (Fig. 2c). The production of hydrogen was maximized when 2.5 mg photocatalyst was added to the catalytic system. By contrast, with larger amounts of photocatalyst, the amount of hydrogen in fact slightly decreased. In addition, hydrogen production activity is well known to be associated with pH. Therefore, a series of experiments were performed with the pH ranging from 0 to 14. The resulting amounts of hydrogen evolution are shown in Fig. S7. In acid medium, the conversion and selectivity were affected only slightly in comparison with neutral pH. However, under alkaline conditions, the conversion rate decreased heavily while the selectivity was slightly increased (Fig. 2d). The possible reason for the reduced hydrogen production in alkaline environments is the low concentration of hydrogen ions, which suppresses hydrogen generation.

^{1}H NMR spectra of reactant and product at various times are shown in Fig. S5 and Fig. 3. The characteristic peak at 9.95 ppm for –CHO of 4-methyl benzaldehyde became increasingly prominent, whereas the peak at 5.10 ppm, corresponding to group –OH, weakened as the reaction time was prolonged. After 15 h of irradiation, the ^{1}H NMR spectrum (top in Fig. 3) displayed a weak peak at 12.8 ppm, corresponding to –COOH. 4-Methyl benzoic acid (m/z 135.0452) was detected by mass spectral analysis at this point in time (Fig. S8†), and the subsequent reaction was very slow. To study the selectivity of products, 4-methoxybenzyl alcohol was chosen as reaction substrate because of the distinct peaks of its products in the aromatic region. As shown in Fig. S9 and S10, the main product is 4-methoxybenzaldehyde, and the byproducts include benzhydrol, benzoyl and benzoin. However, benzoic acid was not found after 5 h irradiation. In the above-mentioned isotope labeling experiment, the holes generated in the photocatalyst under light irradiation were able to oxidize OH^- of H_2O to produce hydroxyl radicals. Subsequently, benzyl alcohol was attacked by the hydroxyl radicals to yield hydroxybenzyl radicals, which may undergo coupling to hydrobenzoin. However, the hydrobenzoin is easily oxidized to form benzoyl and benzoin.[11]

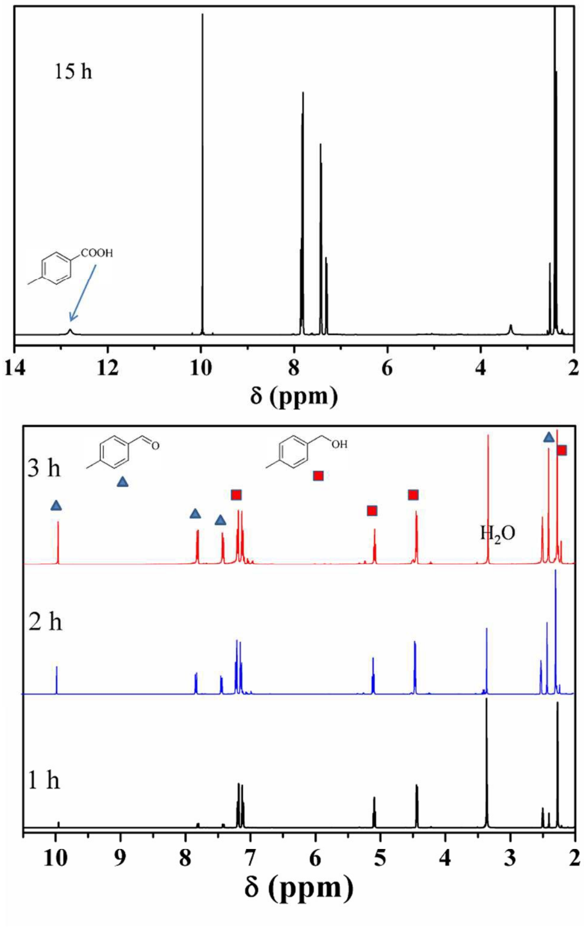

Fig. 3 ^{1}H NMR spectra of 4-methylbenzyl alcohol after various irradiation times.

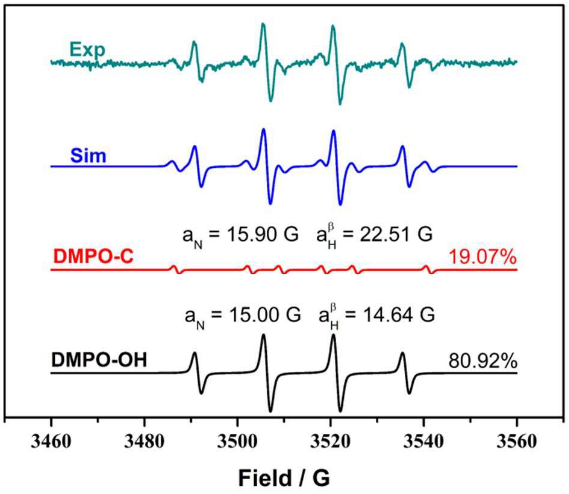

Fig. 4 Exp is the result of the ESR experiment. Sim represents the simulation of the experiment. DMPO-C and DMPO-OH are captured carbon free radicals and hydroxyl free radicals, respectively. Reaction conditions: 2.5 mg CoP/CdS (5 wt%), 5 mL of water, 4-methylbenzyl alcohol (0.1 mmol), at room temperature, irradiation for 15 min.

To gain mechanistic insight into the photocatalytic oxidation process, an ESR spin-trapping experiment was performed, using the trapping agent DMPO (dimethyl pyridine *N*-oxide). In the dark, no free radical signal peak was observed (Fig. S11†). However, significant peaks appeared under white LED irradiation (Fig. 4), the changes of signal intensity with irradiation time were depicted Fig. S11. By computer simulation, the peak was resolved into two sets of peaks with a calculated intensity ratio of approximately 1:4, indicating that they arose from both carbon free radicals and hydroxyl free radicals. In a separate experiment, 1 equivalent of TEMPO (2,2,6,6-Tetramethyl-1-piperidinylox, 0.1 mmol) was added

View Article Online
DOI: 10.1039/C8CY00138C

into the photocatalytic system as a free radical quencher. After 5 h visible-light irradiation, no measurable product was found, except for the original substrate and TEMPO, by NMR spectroscopy and mass spectrometry (Fig. S12†). This further verifies that the photocatalytic oxidation of arylalcohols was driven by a free radical reaction. Therefore, formation of benzhydrol may occur via the decarboxylation of the byproduct benzoic acid to form aryl radicals, which then reacted with hydroxybenzyl radicals to produce benzhydrol via C-C coupling. In addition, a set of free radical quenching experiments was also conducted by employing EDTA-2Na and *tert*-butyl alcohol as quenching agents for holes and hydroxyl radicals, respectively (Table S1†). The conversion was reduced from 88.0% to 3.2% under conditions of hydroxyl radical quenching. This result is consistent with the outcome of the ESR experiment, indicating that hydroxyl radicals are the main active species. Based on the above analysis, a likely mechanism for the complete reaction process is as follows. First, electrons are excited from the valence band to the conduction band of CdS under visible-light irradiation. The excited electrons are delivered to the cocatalyst CoP, where they are combined with hydrogen ions to generate hydrogen gas. Free hydroxyl ions supply electrons into the holes in the valence band to produce the main active species, hydroxyl radicals. Through the action of hydroxyl radicals and holes with substrates, α-H atom is abstracted from benzyl alcohol to create hydroxybenzyl radicals. The hydroxybenzyl radicals are then transformed to aromatic aldehydes by four possible pathways: hydrogen extraction reaction (Eqn (1)), hole oxidation (Eqn (2)), disproportionation (Eqn (3)) and electron transport to the conduction band (Eqn (4)). Based on the results attained, it was tentatively suggested that pathway (1) dominated the photocatalytic oxidative reaction. In addition, byproducts are generated through free radical coupling reactions.

$$\mathrm{Ar\dot{C}H-OH + \dot{O}H \rightarrow ArCHO + H_2O} \qquad (1)$$

$$\mathrm{Ar\dot{C}H-OH + h^+ \rightarrow ArCHO + H^+} \qquad (2)$$

$$\mathrm{2\ Ar\dot{C}H-OH \rightarrow ArCHO + ArCH_2OH} \qquad (3)$$

$$\mathrm{Ar\dot{C}H-OH \rightarrow ArCHO + e^- + H^+} \qquad (4)$$

Other benzyl alcohols with different substituents were introduced into this catalytic system, and the rates of substrate transformation and hydrogen evolution were determined by ^{1}H NMR and GC analysis (Table 1, Fig. S13†). The substrates differed widely in their conversion rates, which can be partially ascribed to the solubility of the reactants in water. However, the substituent groups also had a large direct influence on the conversion. The reaction degree increased with electron-donating substituents, which increase the electron density of the substrate, making it more easily oxidized. Comparing entries 5 and 6, the oxidation rate of diphenyl methanol was faster than that of methyl benzyl alcohol, which can be attributed to the conjugation effect. The stability of the CoP/CdS hybrid catalyst was also investigated. The conversion dropped to 66.2% from 88.0% after 3 consecutive cycles (Fig. S14†), but the catalytic activity was recovered by adding 2 mg CdS into the system. This reveals that CdS is susceptible to photocorrosion during long-term irradiation (Fig. S15†).

Table 1 Catalytic oxidation of benzyl alcohols with different substituents[a]

Entry	Substrate	Main product	Conv. (%)	Sel. (%)	Yield (%)	Theoretical H_2 (μmol)	Actual H_2 (μmol)
1	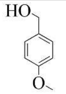	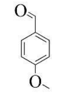	84.3	84.1	70.9	95.5	107.3
2	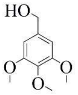	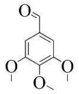	89.4	>99	88.5	100.7	110.7
3	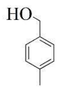	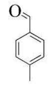	88.0	80.5	70.9	98.1	109.1
4	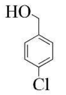	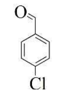	39.6	82.5	32.7	45.9	51.91
5	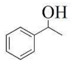	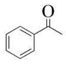	30.3	92.1	27.9	45.7	50.55
6	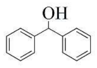	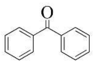	37.4	84.0	31.4	50.1	54.43

[a] Reaction conditions: 2.5 mg CoP/CdS (5 wt%), 5 mL water, substrate (0.1 mmol), visible light irradiation 5 h, at room temperature.

4. Conclusions

In summary, we have constructed a noble-metal-free system for visible-light-catalyzed oxidation of arylalcohols to aromatic aldehydes. The hybrid photocatalytic system comprises CoP as cocatalyst combined with CdS. The reaction is accomplished in water, and accompanied by hydrogen evolution. The observed amounts of H_2 are much more thanthe chemical equivalent of hydrogen gas calculated by producted aldehydes or ketones and byproducts. Mechanistic study revealed that hydroxyl free radicals, generated by photocatalytic water splitting, are the driving species for the reaction, and water acts as a hydrogen source confirmed by isotope labeling experiment. The system developed here meets the requirements of green chemistry and is more atom-economical than existing methods.

Conflicts of interest

There are no conflicts to declare.

Acknowledgements

This work was financially supported by the Natural Science Foundation of China (21267025, 21273257, 21367026 and 21371175) and the Strategic Priority Research Program of the

View Article Online
DOI: 10.1039/C8CY00138C

Chinese Academy of Sciences (XDB17030300) for funding support.

Notes and references

1 S. Garbarino, D. Ravelli, S. Protti and A. Basso, *Angew. Chem. Int. Ed.*, 2016, **55**, 15476–15484.
2 L. J. Shen, S. J. Liang, W. M. Wu, R. W. Liang and L. Wu, *J. Mater Chem. A*, 2013, **1**, 11473–11482.
3 Y. Xu, Z. C. Fu, S. Cao, Y. Chen and W. -F. Fu, *Catal. Sci. Technol.*, 2017, **7**, 587–595.
4 A. Fujishima and M. Honda, *Nature*, 1972, **238**, 37–38.
5 A. Tanaka, K. Hashimoto and H. Kominami, *Chem. Commun.*, 2011, **47**, 10446–10448.
6 D. B. Chao and W. -F. Fu, *Chem. Commun.*, 2013, **49**, 3872–3874.
7 F. Z. Su, S. C. Mathew, G. Lipner, X. Z. Fu, M. Antonietti, S. Blechert and X. C. Wang, *J. Am. Chem. Soc.*, 2010, **132**, 16299–16301.
8 S. Yurdakal, G. Palmisano, V. Loddo, V. Augugliaro and L. Palmisano, *J. Am. Chem. Soc.*, 2008, **130**, 1568–1569.
9 G. Palmisano, S. Yurdakal, V. Augugliaro, V. Loddo and L. Palmisano, *Adv. Synth. Catal.*, 2007, **349**, 964–970.
10 S. Yurdakal,G. Palmisano,V. Loddo,O. Alagöz,V. Augugliaro andL. Palmisano, *Green Chem.*, 2009, **11**, 510–516.
11 T. Mitkina, C. Stanglmair, W. Setzer, M. Gruber, H. Kisch and B. König, *Org. Biomol. Chem.*, 2012, **10**, 3556–3561.
12 Y. Zhang, L. H. Lin, B. Wang and X. C. Wang, *Angew. Chem. Int. Ed.*, 2015, **54**, 12868–12884.
13 L. Su, X. Ye, S. Meng, X. Fu and S. Chen, *Appl. Surf. Sci.*, 2016, **384**, 181–174.
14 S. Meng, X. Ye, X. Ning, M. Xie, X. Fu and S. Chen, *Appl. Catal. B: Environ.*, 2016, **182**, 356–368.
15 M. Qamar, M. O. Fawakhiry, A. -M. Azad, M. I. Ahmed, A. Khan and T. A. Saleh, *RSC Adv.*, 2016, **6**, 71108–71116.
16 S. Samanta, S. Khilari, D. Pradhan and R. Srivastava, *ACS Sustainable Chem. Eng.*, 2017, **5**, 2562–2577.
17 J. Ding, W. Xu, H. Wan, D. Yuan, C. Chen, L. Wan, G. Guan and W. L. Dai, *Appl. Catal. B: Environ.*, 2018, **221**, 626–634.
18 M. Bellardita, E. I. García-López, G. Marcì, I. Krivtsov, J. R. García and L, Palmisano, *Appl. Catal. B: Environ.*, 2018, **220**, 222–233.
19 S. Meng, X. Ning, S. Chang, X. Fu, X. Ye and S. Chen, *J. Catal.*, 2018, **357**, 247–256.
20 J. Zhao, X. Ke, H. Liu, Y. Huang, C. Chen, A. Bo,X. Sheng and H. Zhu, *Part. Part. Syst. Charact.*,2016, **33**, 628–634.
21 X. Xu, R. Liu, Y. Cui, X. Liang, C. Lei, S. Meng, Y. Ma, Z. Lei, Z. Yang, Appl. Catal. B: Environ., 2017, 210, 484–494.
22 Z. Wu, X. Huang, H. Zheng, P. Wang, G. Hai, W, Dong and G. Wang, Appl. Catal. B: Environ., 2018, 224, 479–487
23 A. Tanaka, K. Hashimoto and H. Kominami, *J. Am. Chem. Soc.*, 2012, **134**, 14526–14533.
24 M. Qamar, R. B. Elsayed, K. R. Alhooshani, M. I. Ahmed and D. W. Bahnemann, *ACS Appl. Mater. Interfaces*, 2015, **7**, 1257–1269.
25 F.J. López-Tenllado, S. Murcia-López, D.M. Gómez, A. Marinas, J.M. Marinas, F.J. Urbano, J.A. Navío, M.C. Hidalgo and J.M. Gatica, *Appl. Catal. A: Gen.*, 2015, **505**, 375–381.
26 Y. Liu, P. Zhang, B. Z. Tian and J. L. Zhang, *ACS Appl. Mater. Interfaces*, 2015, **7**, 13849–13858..
27 P. Zhang, Y. Liu, B. Z. Tian, Y. S. Luo and J. L. Zhang, *Catal. Today*, 2017, **281**, 181–188.
28 H. J. Yan, J. H. Yang, G. J. Ma, G. P. Wu, X. Zong, Z. B. Lei, J. Y. Shi and C. Li, *J. Catal.*, 2009, **266**, 165–168.
29 G. Y. Yu, X. Wang, J. G. Cao, S. J. Wu, W. F. Yan and G. Liu, *Chem. Commun.*, 2016, **52**, 2394–2397.
30 W. Z. Gao, Y. Xu, Y. Chen and W. F. Fu, *Chem. Commun.*, 2015,**51**, 13217–13220.
31 S. Cao, Y. Chen, C. J. Wang, X. J. Lv and W. -F. Fu, *Chem. Commun.*, 2015, **51**, 8708–8711.
32 P. Jiang, Q. Liu, C. J. Ge, W. Cui, Z. H. Pu, A. M. Asiri and X. P. Sun, *J. Mater. Chem. A*, 2014, **2**, 14634–14640.

View Article Online
DOI: 10.1039/C8CY00138C

Graphical abstract

Hydroxyl free radicals generated by visible-light-catalyzed water splitting over CoP/CdS drive the oxidation of arylalcohols with hydrogen evolution